Наносистеми, наноматеріали, нанотехнології
Nanosistemi, Nanomateriali, Nanotehnologii
2024, т. 22, № 1, сс. 13–30
https://doi.org/10.15407/nnn.22.01.013

PACS numbers: 61.66.Fn, 64.75.Nx, 65.40.Ba, 81.30.Dz, 81.40.Cd, 82.33.Pt, 82.60.Lf

Predicting the Thermodynamic Stability of $(Gd_{1-x}Ln_x)_2SiO_5$ and $(Lu_{1-x}Ln_x)_2SiO_5$ Solid Solutions of the $P2_1/c$ Space Group

E. I. Get'man[1], O. Yu. Mariichak[1], L. I. Ardanova[2], and S. V. Radio[1]

[1]*Vasyl' Stus Donetsk National University,*
21, 600th Anniversary Str.,
UA-21027 Vinnytsia, Ukraine
[2]*Department of Chemistry and Geology,*
Minnesota State University,
56001 Mankato, Minnesota, USA

Within the framework of V. S. Urusov's crystal-energy theory of isomorphous substitutions, the mixing energies (interaction parameters) and critical decomposition (stability) temperatures are calculated for the $(Gd_{1-x}Ln_x)_2SiO_5$ systems, where Ln represents rare-earth elements (REEs) or yttrium. The values of the total mixing energies are determined mainly by contributions arising from the difference in sizes of the substituting structural units. The contributions due to differences in the degree of ionicity of the chemical bond between the components are significantly smaller and can be neglected in most cases. Diagrams of the thermodynamic stability of systems $(Gd_{1-x}Ln_x)_2SiO_5$ and decomposition domes of the $(Gd_{1-x}Ln_x)_2SiO_5$ and $(Lu_{1-x}Ln_x)_2SiO_5$ systems are presented, which allow for graphical prediction of decomposition temperatures of solid solutions within the specified substitution limits, equilibrium substitution limits at a given temperature, and ranges of thermodynamic stability for solid solutions. The predictions of thermodynamic stability are consistent with experimental data previously reported in the literature for solid solutions based on doped gadolinium oxyorthosilicate. The gadolinium oxyorthosilicate solid solutions, which exhibit luminescent, scintillation, and other practically important properties, due to their very low critical decomposition temperatures and a wide temperature range of thermodynamic stability compared to solid solutions of oxyorthosilicate of other REEs, can find practical applications as nanomaterials.

У рамках кристалоенергетичної теорії ізоморфних заміщень В. С. Урусова розраховано енергії змішання (параметри взаємодії) та критичні температури розпаду (стабільности) у системах $(Gd_{1-x}Ln_x)_2SiO_5$, де Ln — рідкісноземельні елементи (РЗЕ) й ітрій. Величини сумарної енергії

змішання визначаються в основному внесками, зумовленими ріжницею розмірів структурних одиниць, які заміщаються. Величини внесків за рахунок відмінностей у ступені йонности хемічного зв'язку компонентів істотно менші та здебільшого ними можна нехтувати. Представлено діяграму термодинамічної стабільности системи $(Gd_{1-x}Ln_x)_2SiO_5$ та бані розпаду систем $(Gd_{1-x}Ln_x)_2SiO_5$ і $(Lu_{1-x}Ln_x)_2SiO_5$, які уможливлюють графічно передбачати температури розпаду твердих розчинів за заданих границь заміщення, рівноважні границі заміщення за заданої температури й області термодинамічної стабільности твердих розчинів. Результати прогнозування термодинамічної стабільности не суперечать експериментальним даним, раніше наведеним у літературі для твердих розчинів на основі допованого Ґадолінію оксиортосилікату. Тверді розчини Ґадолінію оксиортосилікату, які мають люмінесцентні, сцинтиляційні й інші практично важливі властивості, внаслідок дуже низьких критичних температур розпаду та дуже широкого температурного інтервалу термодинамічної стабільности в порівнянні з твердими розчинами оксиортосилікатів інших РЗЕ можуть знайти практичне застосування в якості наноматеріялів.

Key words: solid solution, mixing energy, isomorphous substitutions, complex oxide systems, oxyorthosilicate, rare-earth elements, gadolinium, yttrium.

Ключові слова: твердий розчин, енергія змішання, ізоморфні заміщення, складнооксидні системи, оксиортосилікати, рідкісноземельні елементи, Ґадоліній, Ітрій.

(Received 23 June, 2023)

1. INTRODUCTION

Gadolinium oxyorthosilicate (Gd_2SiO_5), doped with rare-earth elements (REEs), can be utilized as phosphors, gamma radiation detectors for high-energy physics in nuclear physics, single-crystal scintillators, and in the latest generation of scintillation detectors in positron emission tomography (PET). It is also employed for monitoring radiation levels in test sites and the operation of pulsed electron guns and electron beam technology, as well as in oil well logging [1–5]. This is due to the complex set of physicochemical and electrophysical properties possessed by Gd_2SiO_5, including relatively high density, chemical and thermal stability, non-hygroscopicity, and radiation resistance [1]. It exhibits a high absorption coefficient, good uniformity of scintillation characteristics [2], sufficient radiation intensity, high potential as gamma radiation detectors [3], excellent energy resolution, rapid decay, and superior homogeneity of scintillation blinking [4]. Rare-earth elements Ce, Eu, Tb, Dy, and Yb are commonly used as dopants, while La, Gd, Lu, and Y serve as second components in the crystalline ma-

trices of mixed gadolinium oxyorthosilicates. Consequently, intensive research has been conducted in recent years to investigate the effects of isomorphous substitutions on various properties of solid solutions of REEs oxyorthosilicates based on Gd_2SiO_5, including mixed oxyorthosilicates, as described in works [6–18].

However, it is not always considered that solid solutions synthesized at high temperatures are prone to decomposition upon cooling within the region of thermodynamic instability, leading to changes in phase composition and properties [19–21]. This can result in material degradation and a lack of reproducibility of properties during practical application.

Therefore, it is desirable to evaluate the thermodynamic stability of solid solutions in the corresponding systems before their synthesis and properties investigation, considering the synthesis conditions, expected operating conditions, and even storage conditions. However, the physicochemical foundations for synthesizing of REEs oxyorthosilicates solid solutions, such as phase diagrams and their thermodynamic stability, have been scarcely studied to date.

The experimental determination of substitution limits by x-ray phase analysis (x-ray diffraction—XRD) using the 'annealing and hardening' method, and the subsequent evaluation of the stability regions of solid solutions, is complicated by the difficulty of reaching equilibrium at low temperatures due to slow diffusion rates in the solid phase and the possibility of partial decomposition upon cooling from high temperatures. Additionally, XRD may provide limited information when the components have nearly identical sizes of substituting structural units, or in the case of spinodal decomposition of the solid solution [19–21], or in the case of nanosized particles in the studied samples, which can lead to broadening and overlapping of x-ray reflections.

Insufficient information about the stability regions of solid solutions forces researchers to choose the composition of matrices and modifying additives (dopants) based either on analogous systems or through a 'trial-and-error' approach. This can result in excessive consumption of expensive reagents and prolonged research duration.

Therefore, it is rational to employ not only experimental but also computational methods that are free from the aforementioned limitations. As an example of such an approach, we can refer to studies [22, 23], where the synthesis conditions for samples of the $Y_{1-x}Sc_xPO_4$ system were determined based on computational results obtained for this system in [24].

Considering the above, the aim of this study was to predict the regions of thermodynamic stability for solid solutions of gadolinium oxyorthosilicates $(Gd_{1-x}Ln_x)_2SiO_5$ and lutetium oxyorthosilicates

$(Lu_{1-x}Ln_x)_2SiO_5$ with the space group $P2_1/c$.

The choice of gadolinium oxyorthosilicate as one of the components in the $(Gd_{1-x}Ln_x)_2SiO_5$ systems is justified by the fact that it does not have inherent absorption bands in the visible spectrum and is expected to form wide regions of solid solutions with oxyorthosilicates of most REEs at relatively low temperatures due to the similarity in ionic radii [25] and electronegativity values [26] between gadolinium and other REEs. According to [19], the prediction of substitution limits is based on 1 mole of substituting cation, and the anionic sublattice of oxyorthosilicates contains SiO_4^{4-} and O^{2-} anions not directly bonded to Si atoms [27]. Therefore, the composition of the oxyorthosilicate is presented as a pseudobinary compound $Gd[(SiO_4)_{0.5}O_{0.5}]$, and the corresponding solid solutions are denoted as $(Gd_{1-x}Ln_x)[(SiO_4)_{0.5}O_{0.5}]$, while the traditional formula notation of gadolinium oxyorthosilicate Gd_2SiO_5 is used in the article text.

2. CALCULATION METHODOLOGY AND INITIAL DATA

In the developed by V. S. Urusov crystal-energy theory of isomorphous substitutions [19–21], the main challenge in determining the limits of isomorphous substitutions and regions of thermodynamic stability is finding the mixing energy. Once the mixing energy is known, the substitution limit (x) can be calculated for a given decomposition (stability) temperature (T_d), or the decomposition temperature can be determined for a given substitution limit, allowing for the determination of regions of thermodynamic stability. The Becker equation in the regular solid solution approximation (Eq. (1) can be used for these calculations [28]:

$$-\frac{1-2x}{\ln\frac{x}{1-x}} = R_g T_d / Q . \tag{1}$$

The critical decomposition temperatures (T_{cr}) in this case are calculated using Eq. (2) [19]:

$$T_{cr} = Q/(2kN), \tag{2}$$

where x is the substitution limit; R_g is the universal gas constant; Q is the mixing energy; k is the Boltzmann constant; N is Avogadro's number. In both cases, the value of Q is expressed in cal/mol [19].

The Becker equation can be used because the size parameter (Table 1) does not exceed 0.1 [19]. The size parameter was calculated based on the volumes of unit cells: $\delta = (V^{1/3}_{Ln_2SiO_5} - V^{1/3}_{Gd_2SiO_5})/V^{1/3}_{min}$ [19], where V_{min} is the volume of the smaller unit cell.

TABLE 1. Calculation of mixing energies of oxyorthosilicates $(Gd_{1-x}Ln_x)_2SiO_5$, Ln = La–Lu, Y, with the $P2_1/c$ space group.

Ln	V^*, Å^3	δ	C	Q_R, kJ/mol	χ_{Ln}	ε	Δε	Q_ε, kJ/mol	Q, kJ/mol
La	465.2	0.03963	114.92	21.110	1.327	0.724	0.012	1.955	23.065
Ce	455.2	0.03212	114.08	13.770	1.348	0.720	0.008	0.869	14.639
Pr	445.1	0.02444	113.04	7.900	1.374	0.716	0.004	0.217	8.117
Nd	439.3	0.01996	112.72	5.254	1.382	0.714	0.002	0.054	5.308
Pm	431.9	0.01421	112.36	2.655	1.391	0.712	0	0	2.655
Sm	424.4	0.00830	111.6	0.900	1.410	0.708	0.004	0.217	1.117
Eu	417.9	0.003130	110.68	0.127	1.433	0.704	0.008	0.869	0.996
Gd	414.0		112.56		1.386	0.712			
Tb	409.2	0.003895	111.6	0.198	1.410	0.708	0.004	0.217	0.415
Dy	404.0	0.008183	110.96	0.869	1.426	0.706	0.006	0.489	1.358
Ho	397.5	0.013649	110.68	2.412	1.433	0.704	0.008	0.869	3.281
Er	395.6	0.0152695	110.48	3.014	1.438	0.703	0.009	1.100	4.114
Tm	389.7	0.020367	109.8	5.329	1.455	0.700	0.012	1.955	7.284
Yb	387.0	0.022735	108.84	6.582	1.479	0.695	0.017	3.925	10.507
Lu	384.0	0.0253914	110.76	8.355	1.431	0.705	0.007	0.665	9.010
Y	397.4	0.0137334	112.56	2.480	1.340	0.722	0.010	0.680	3.160

*Note: The unit cell volumes of cerium and promethium oxyorthosilicates are determined as the arithmetic means of the unit cell volumes of lanthanum and praseodymium oxyorthosilicates, as well as neodymium and samarium oxyorthosilicates, respectively.

The use of unit cell volumes for the calculation is justified by the lack of available literature providing interatomic distances for the low-temperature modification Ln_2SiO_5, as seen in [29–31]. Furthermore, the authors in [29], who initially described the $P2_1/c$ space group for Ln_2SiO_5, do not present cell parameters for Lu_2SiO_5. Therefore, we determined the volume of the unit cell of the low-temperature modification Lu_2SiO_5 (approximately 384 Å^3) through extrapolation of the unit cell volumes of Ln_2SiO_5 based on the ionic radii of REEs [32].

Since the components of the considered systems are isostructural [27, 29], the equation 3 for calculating the mixing energy (Q) consists of two contributions arising from the difference in sizes of substituting structural units (Q_δ) and the difference in the ionicity of the chemical bond between the components (Q_ε) [19].

$$Q = Q_\delta + Q_\varepsilon = Cmnz_m z_x \delta^2 + \frac{1390 m z_m z_x \alpha(\Delta\varepsilon)^2}{2R} \text{ [kJ/mol]}. \quad (3)$$

It should be noted that at temperatures above 1173–1373 K, the components of systems involving high-temperature modifications of oxyorthosilicates in the series of REEs from Dy to Lu and from La to Tb are not isostructural (the $P2_1/c$ space group is observed for oxyorthosilicates from La to Tb, while the $B2/b$ space group is observed for Dy to Lu oxyorthosilicates) [27]. Therefore, in this case, it is also necessary to consider a third contribution to the mixing energy due to the enthalpy of the polymorphic transition $P2_1/c \rightarrow B2/b$ [19], for which, according to our data, there is no information available in the literature.

In equation 3, the value of C is a constant calculated from the expression $C = 20(2\Delta\chi + 1)$ [21], where $\Delta\chi$ represents the electronegativity difference between the cations [26] and the anion [33] in the pseudobinary approximation of the structure (Table 1). The choice of the χ scale [26], unlike scales used by other authors, is based on the fact that χ values vary with periodicity, increasing in the series Ce^{3+}–Eu^{3+} from 1.348 to 1.433 and in the series Gd^{3+}–Yb^{3+} from 1.386 to 1.479, with a sharp decrease during the transitions Eu^{3+}–Gd^{3+} from 1.433 to 1.386 and Yb^{3+}–Lu^{3+} from 1.479 to 1.431. These variations are due to the peculiarities of the electronic shell filling of REEs. The lanthanum has a free 4f shell, europium and gadolinium have a half-filled 4f shell (7 electrons), and ytterbium and lutetium have a completely filled 4f shell (14 electrons). In the transition from Eu to Gd and from Y to Lu, as well as for La, the first electron appears on the 5d sublevel.

m is the number of formula units in the pseudobinary approximation of the structure $(Gd_{1-x}Ln_x)[(SiO_4)_{0.5}O_{0.5}]$ is calculated per 1 mole of substituting structural unit $(1 + 0.5 + 0.5 = 2)$; n—the coordina-

tion number of the substituting structural unit in the pseudobinary approximation of the structure (in the first cation position, $n = 7{:}6SiO_4^{4-}$ tetrahedra and one O^{2-} ion; in the second position, $n = 6{:}3SiO_4^{4-}$ tetrahedra and three O^{2-} ions [27]), *i.e.*, on average, $n = 6.5$; z_m, z_x—the formal charges of the substituting and common structural units in the components: $z_m = 3$, $z_x = 4{\cdot}0.5 + 2{\cdot}0.5 = 3$; δ—the size parameter, calculated for each system based on the volumes of unit cells provided in [27, 29]; ε—the degree of ionicity of the chemical bond were determined based on the electronegativity difference χ between the REE cations and the anion, as provided in [26, 33]. The value of χ for the SiO_4^{4-} radical was adopted as χ of the oxide anion, following the recommendation [34], and it was taken as 3.7 [33].

α is the reduced Madelung constant, equal to 1.9, was calculated using the Hoppe formula [35]: $(\alpha/n)^2 + \alpha = 1.81$;

R is the average cation–anion interatomic distance in the pseudobinary approximation, was calculated for one of the previously studied structures of this structural type—$Gd[(SiO_4)_{0.5}O_{0.5}]$ [27]. The distances between the cation and the tetrahedral anion were taken into account as the sum of the distances (Gd–O + Si–O) and the distance between the cation and oxygen (Gd–O) not bonded to a Si atom for both positions of gadolinium [27]. For the first position: the cation is surrounded by 6 tetrahedra + 1 oxygen, resulting in an average distance of $[6{\cdot}(2.49 + 1.63) + 2.35]/7 = 3.86$Å; for the second position: the cation is surrounded by 3 tetrahedra + 3 oxygen, resulting in an average distance of $[3{\cdot}(2.39 + 1.63) + 3{\cdot}2.30)]/6 = 3.15$ Å. The average distance, considering both cation positions, is $R = 3.5$ Å. The calculation error for T_{cr} was ±100 K [19].

3. RESULTS OF THE CALCULATIONS AND DISCUSSION

3.1. Mixing Energies of Oxyorthosilicates $(Gd_{1-x}Ln_x)_2SiO_5$

Some initial data and results of the mixing energy calculations are summarized in Table 1 and Fig. 1. As can be seen from the provided data, with an increase in the atomic number of the REEs, the contributions to the total mixing energy due to differences in the sizes of substituting structural units Q_R (Fig. 1) smoothly vary in the series of systems from $(Gd_{1-x}La_x)_2SiO_5$ to $(Gd_{1-x}Eu_x)_2SiO_5$, decreasing significantly from 21.110 to 0.127, and then increasing from 0.198 to 8.355 kJ/mol in the series of solid solutions from $(Gd_{1-x}Tb_x)_2SiO_5$ to $(Gd_{1-x}Lu_x)_2SiO_5$.

Such variation in the Q_R mixing energy is caused by the fact that in the series of systems with La–Eu oxyorthosilicates, the differences between the crystal radii of the ions in the La–Eu range

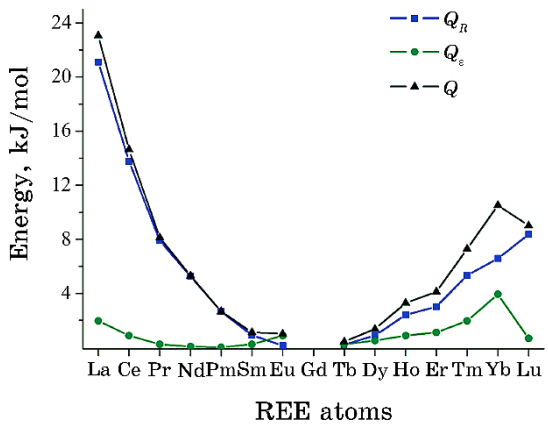

Fig. 1. Dependences of the calculated contributions to the mixing energies of solid solutions Q_R (■) and Q_ε (●), as well as for Q (▲), in the systems $(Gd_{1-x}Ln_x)_2SiO_5$ for the La–Lu series.

(1.300–1.206 Å) and gadolinium (1.193 Å) decrease, while in the series of systems with Tb–Lu oxyorthosilicates (1.180–1.117 Å), on the contrary, they increase. This is because the crystal radius of gadolinium (1.193 Å) is very close to the radius of europium and terbium (1.206 and 1.180 Å). Here and further, the crystal ionic radii of cations are given according to *R*. Shannon [25] for a coordination number of 8.

The value of the total mixing energy Q is mostly determined by the contribution due to differences in the sizes of the substituting structural units Q_R, except for the systems $(Gd_{1-x}Tm_x)_2SiO_5$ and $(Gd_{1-x}Yb_x)_2SiO_5$, where the contribution Q_ε is comparable to the corresponding values of Q_R. The minimal mixing energies of the systems in the series $(Gd_{1-x}Sm_x)_2SiO_5$–$(Gd_{1-x}Dy_x)_2SiO_5$ are due to very close values of the crystal ionic radii and electronegativities of the respective REEs and gadolinium. The maxima in the contributions Q_ε for $(Gd_{1-x}La_x)_2SiO_5$, $(Gd_{1-x}Eu_x)_2SiO_5$, and $(Gd_{1-x}Yb_x)_2SiO_5$ are due to the above-mentioned electronic shell structures of lanthanum, europium, and ytterbium.

3.2. Limits of Isomorphous Substitutions in Oxyorthosilicates $(Gd_{1-x}Ln_x)_2SiO_5$

The decomposition temperatures of limited series of solid solutions (Table 2) were calculated based on the given substitution limits at $x = 0.01$, 0.03, 0.09, and 0.20 using equation (1), while the critical decomposition (stability) temperatures were determined at $x = 0.50$ using Eq. (2).

TABLE 2. Decomposition temperatures of solid solutions of oxyorthosilicates $(Gd_{1-x}Ln_x)_2SiO_5$ for $x = 0.01$, 0.03, 0.09, and 0.20, and critical decomposition temperatures (T_{cr} [K] for $x = 0.50$).

Ln	Decomposition temperatures, K				
	$x = 0.01$	$x = 0.03$	$x = 0.09$	$x = 0.20$	$x = 0.50$ (T_{cr})
La	587	745	976	1178	1377
Ce	373	473	620	757	874
Pr	207	262	344	415	485
Nd	135	171	225	271	316
Pm	68	86	109	137	158
Sm	28	36	46	57	67
Eu	25	32	41	51	59
Tb	11	13	18	21	25
Dy	35	44	56	69	81
Ho	84	106	135	168	196
Er	105	133	174	210	246
Tm	186	235	308	377	435
Yb	268	339	445	543	628
Lu	229	291	381	466	538
Y	81	102	134	163	190

Based on the calculated values of the decomposition temperatures, their dependences on the REEs numbers were plotted (Fig. 2).

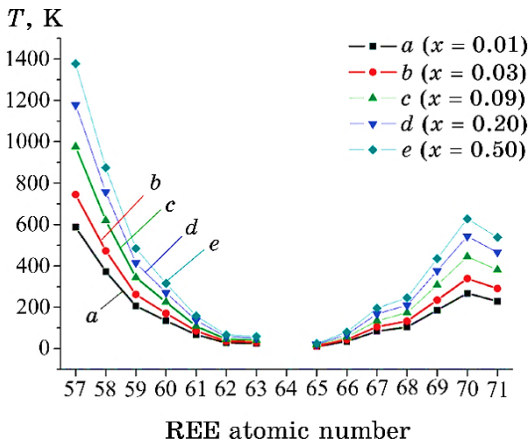

Fig. 2. Dependences of the calculated decomposition temperatures of solid solutions of oxyorthosilicates $(Gd_{1-x}Ln_x)_2SiO_5$ on the REEs atomic numbers for substitution limits $x = 0.01$ (*a*), $x = 0.03$ (*b*), $x = 0.09$ (*c*), $x = 0.20$ (*d*), and $x = 0.50$ (*e*).

These dependences allow for graphical determination of the equilibrium substitution limits (x) at specified decomposition temperatures (T_d), or the decomposition temperatures for given substitution limits for gadolinium oxyorthosilicate with REEs ranging from La to Lu [24]. The intersection points of an isotherm drawn from a given decomposition temperature and a vertical line drawn from the REE number allows for estimating the composition range within which the substitution limit is located, and interpolation along this vertical line segment between the two closest curves provides the actual substitution limit. To refine the substitution limit, the dependence of calculated decomposition temperatures on the specified composition (decomposition dome) can be plotted for a specific system. The critical decomposition temperatures for unlimited series of solid solutions (Fig. 2, *e*) vary with the REEs numbers in accordance with the changes in the total mixing energy, as predicted by the Becker equation.

3.3. Thermodynamic Stability Regions of $(Gd_{1-x}Ln_x)_2SiO_5$ Solid Solutions

Based on Figure 2, the thermodynamic stability regions of $(Gd_{1-x}Ln_x)_2SiO_5$ solid solutions can be assessed graphically. At temperatures above T_{cr} (curve *e*), the unlimited series of solid solutions are thermodynamically stable across the concentration range of $1.0 > x > 0$. In the region below curve *e*, at temperatures below T_{cr}, the unlimited solid solutions become unstable and can undergo decomposition into phases with limited solubility if the diffusion rate and time are enough for their formation [24]. Solid solutions with x values of 0.01, 0.03, 0.09, and 0.20 are thermodynamically stable in the regions above curves (*a*), (*b*), (*c*), and (*d*), respectively, while they become unstable below these curves.

It should be noted that solid solutions of $(Gd_{1-x}Ln_x)_2SiO_5$ systems have very low critical decomposition temperatures, with 8 out of 15 such systems even below room temperature. Therefore, the latter will exhibit thermodynamic stability over a wide temperature range, ranging from below room temperature to the melting temperatures, which for REEs oxyorthosilicates are in the range of 2170–2320 K [36]. This fact may indicate an advantage of Gd-based oxyorthosilicates solid solution materials in terms of stability of properties and their reproducibility compared to similar materials based on solid solutions of oxyorthosilicates of other REEs such as cerium [37].

For all $(Gd_{1-x}Ln_x)_2SiO_5$ systems, the decomposition temperatures were calculated within the composition range of $1.0 > x > 0$ with a step size of $x = 0.05$, and decomposition domes were plotted (Fig. 3). They allow for a more precise graphical determination of the ther-

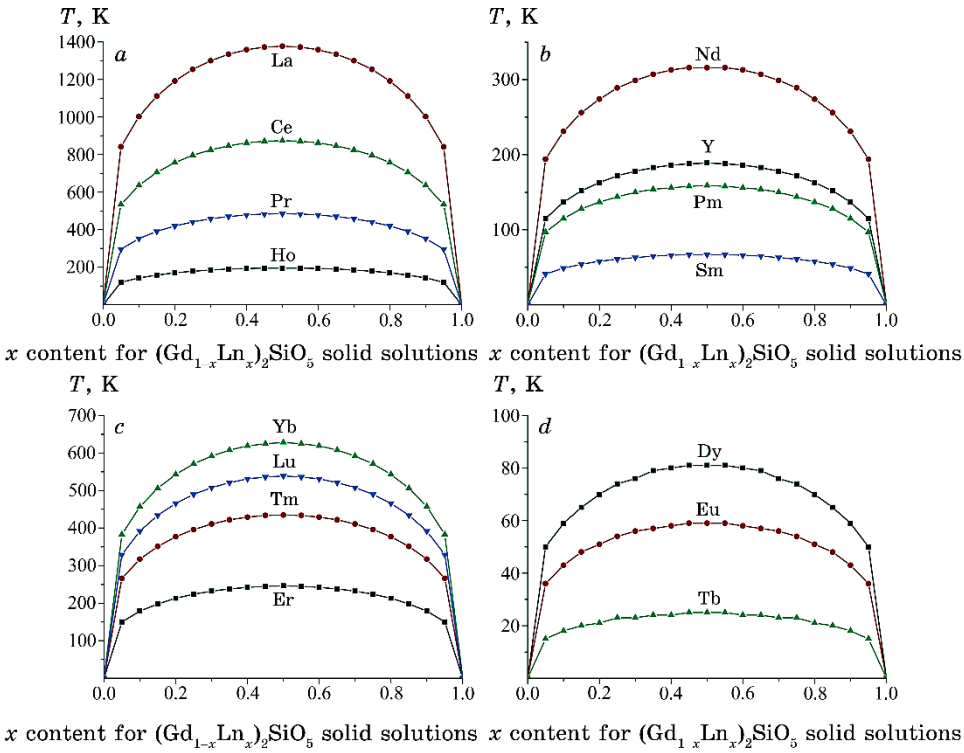

Fig. 3. Decomposition domes for solid solutions of $(Gd_{1-x}Ln_x)_2SiO_5$ oxyorthosilicates: (*a*) Ln = La, Ce, Pr, Ho; (*b*) Ln = Nd, Y, Pm, Sm; (*c*) Ln = Yb, Lu, Tm, Er; (*d*) Ln = Dy, Eu, Tb.

modynamic stability regions, the decomposition temperature for a given limiting composition of the solid solution, or its equilibrium composition at a given decomposition temperature.

4. COMPARISON OF CALCULATION RESULTS WITH LITERATURE DATA

In the literature, there is scarce data available on the thermodynamic stability, substitution limits, and critical decomposition temperatures of solid solution systems based on Gd_2SiO_5. This, of course, hinders the assessment of the reliability of the conducted calculations. However, there are numerous studies on the synthesis temperatures of Gd_2SiO_5 doped with REEs, for example [11, 17, 40–42], and as far as we know, about 15 studies on the synthesis temperatures of mixed oxyorthosilicates [1–4, 6–10, 12–14, 16, 38, 39] (Table 3).

TABLE 3. Comparison of critical decomposition temperatures T_{cr} of solid solutions based on Gd_2SiO_5 oxyorthosilicate with literature data on synthesis temperatures.

Composition [Ref.]	x or %	Synthesis method	Synthesis temperature, K	T_{cr}, K
$Y_{1.92-x}Gd_xSiO_5:Ce_{0.08}$ [6]	0.00, 0.25, 0.50, 0.75	solid phase	1373	190
$(Y_{0.995-x}Gd_xCe_{0.005})_2SiO_5$ [7]	0.05, 0.1, 0.15, 0.20, 0.25, 0.30, 0.35, 0.40	MS&Solgel method + calcination	923 + 1473	190
$(Gd_{1-x}Y_x)_2SiO_5$:Yb5% [8]	0, 0.1, 0.3, 0.5, 0.7, 0.9, 1.0	Czochralski method	Synthesis at 1673 + melting	190
$Gd_{1.99-x}Y_xCe_{0.01}SiO_5$ [9]	0, 0.0995, 0.199	Czochralski method	Synthesis at 1473 + melting	190
$Lu_{2x}Gd_{2-2x}SiO_5$:Ce0.33% [10]	0, 0.2, 0.4. 0.6, 0.8, 1.0	Czochralski method, combined with annealing at 1373 K	1373	538
$Gd_2SiO_5:Ce^{3+}$ [11]	0.5, 1, 2, 5 mol.%	In Na_2CO_3 melt + annealing	Annealing at 1423	874
$Gd_2SiO_5:Dy^{3+}$ [11]	0.2, 1, 2, 5, 10 mol.%	In Na_2CO_3 melt + annealing	Annealing at 1423	81
$Gd_2SiO_5:Eu^{3+}$ [11]	0.5, 1, 2, 5, 10 mol.%	In Na_2CO_3 melt + annealing	Annealing at 1423	59
$Gd_2SiO_5Tb^{3+}$ [11]	0.5, 1, 2, 5, 10 mol.%	In Na_2CO_3 melt + annealing	Annealing at 1423	25
$(Lu_{1-x}Gd_x)_2SiO_5:Ce^{3+}$ 1.5% [12]	0.2, 0.4, 0.5, 0.7	A single-crystal film is formed from a melt-solution of $PbO:B_2O_3$	1273	538

Continuation of **TABLE 3.**

Composition [Ref.]	x or %	Synthesis method	Synthesis temperature, K	T_{cr}, K
$LaGdSiO_5:Dy^{3+}$ 1% [13] multiphase mixture	1 mol.%	by burning urea solution + laser evaporation coating	Annealing at 1273. Improvement of properties	1377
$GdYSiO_5:Dy^{3+}$ [14]	0.025, 0.05, 0.1, 0.25, 0.75, 1.0, 1.5, 2.0, 3.0, 5.0 mol.%	by burning urea solution + laser evaporation coating	Annealing at 1273. Improvement of properties	190
$Gd_2SiO_5:Tb^{3+}$ [15]	2.33, 2.7 mol.%	solid phase	1773	25
$La_{0.5}Gd_{1.5}SiO_5:Dy^{3+}$ [16] two-phase films at all temperatures		by burning urea solution + laser evaporation coating	Substrate temperature 473 + 773, annealing at 1273. Improvement of properties	1377
$Gd_2SiO_5:Eu^{3+}$ [17]	0.1, 0.2, 0.5, 1.0, 1.5, 2.0, 2.5 mol.%	solid phase	1473	59
$Gd_{1.9}Y_{0.1}SiO_5$:0.5% Ce [18]	0.5 mol.%	Czochralski method	1473	190
$La_{0.5}Gd_{1.5}SiO_5:Dy^{3+}$ phases based on Gd_2SiO_5 and La_2SiO_5 with a shift of x-ray reflections [38]		by burning urea solution + laser evaporation coating	Substrate temperature: 673, 773. Time: 15 minutes, 30 minutes, and 50 minutes	1377
$La_{2-x}Gd_xSiO_5:Dy^{3+}$, Pr^{3+} phases based on Gd_2SiO_5 and La_2SiO_5 with a shift of x-ray reflections can be observed in both powders and films, at $x = 0.5$, 1.0, and 1.5 [39]		by burning urea solution + laser evaporation coating	Furnace temperature: 873. Synthesis by flame combustion	1377

Since the dopant content is usually in small quantity or several percent, solid solutions involving it can be thermodynamically stable over a wide temperature range [19]. On the other hand, the amount of the second REE in the mixed oxyorthosilicate matrix typically constitutes tens of percent, which can lead to the decomposition of the solid solution, accompanied by changes in phase composition and properties upon cooling after synthesis and during practical application. For example, mixed crystals of $Lu_{0.4}Gd_{1.6}SiO_5$ annealed after growth have shown improved scintillation emission, higher light output (2.0 times higher than that of Gd_2SiO_5), and good energy resolution [4], highlighting the need to ensure their thermodynamic stability during cooling and practical use.

Comparison of the calculation results with the experimental literature data on synthesis temperatures, as presented in Table 3, indicates that the synthesis of $(Gd_{1-x}Ln_x)_2SiO_5$ oxyorthosilicates solid solution in the majority of studies was conducted within the predicted ranges of thermodynamic stability. This is because the synthesis temperatures were higher than the calculated critical decomposition temperatures. Only in studies [13, 16] and possibly [38, 39], were the synthesis temperatures lower than the calculated critical decomposition temperatures. In other words, the authors carried out the synthesis of solid solution samples at temperatures below the decomposition dome temperatures of the $(Gd_{1-x}La_x)_2SiO_5$ solid solution (Table 3). This resulted in the formation of two-phase solid solutions samples in systems [13, 16, 38, 39], where the interplanar distances of each phase varied with the composition, which is also consistent with the prediction results. Below the decomposition dome, samples in an equilibrium state should not be single-phase.

5. DECOMPOSITION DOMES OF $(Lu_{1-x}Ln_x)_2SiO_5$ SYSTEMS

Previously [32], using the same methodology, we calculated the mixing energies and critical decomposition temperatures of $(Lu_{1-x}Ln_x)_2SiO_5$ systems. However, the decomposition domes were not presented. In addition to the work [32], the decomposition domes of $(Lu_{1-x}Ln_x)_2SiO_5$ systems are shown in Fig. 4.

6. CONCLUSIONS

1. The values of total mixing energies Q decrease in the case of substituting gadolinium with cerium subgroup REEs in the series from La to Eu, and they show a moderate increase when gadolinium is substituted with yttrium subgroup REEs. In both cases, these val-

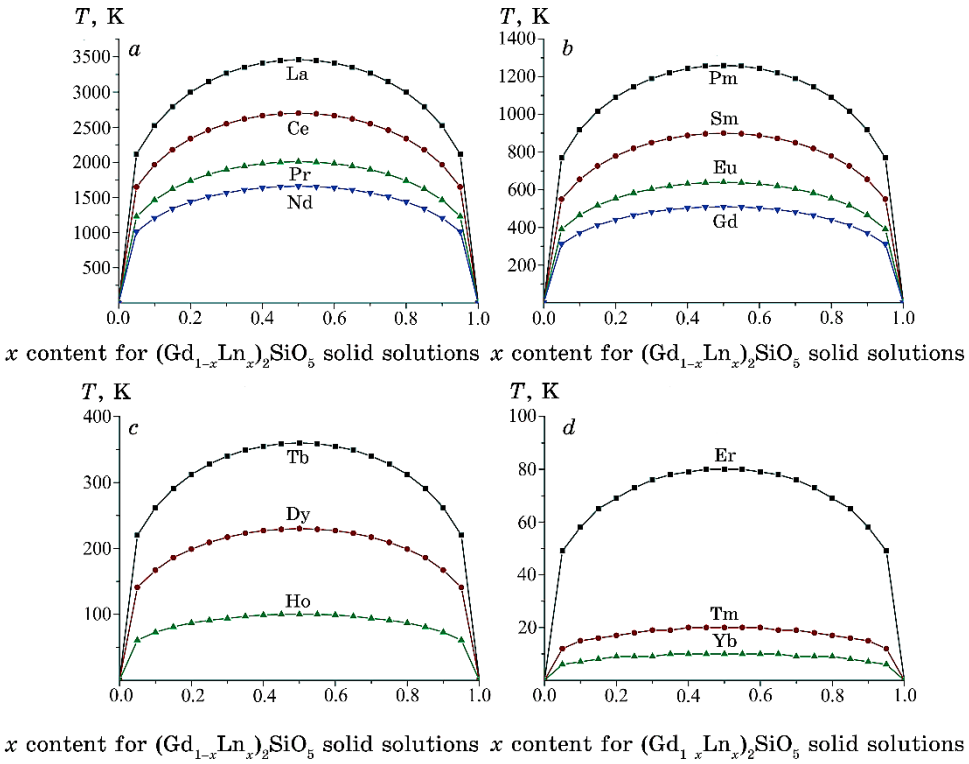

Fig. 4. Decomposition domes of oxyorthosilicates $(Lu_{1-x}Ln_x)_2SiO_5$ solid solutions: (*a*) Ln = La, Ce, Pr, Nd; (*b*) Ln = Pm, Sm, Eu, Gd; (*c*) Ln = Tb, Dy, Ho; (*d*) Ln = Er, Tm, Yb.

ues are mainly determined by contributions arising from the differences in sizes of the substituting structural units Q_R.

2. The contributions arising from the differences in the degree of ionicity of the chemical bond between the components are significantly smaller, and in most cases (except for $(Gd_{1-x}Yb_x)_2SiO_5$ and $(Gd_{1-x}Tm_x)_2SiO_5$ systems), they can be neglected. The insignificant maxima in the Q_ε contributions for $(Gd_{1-x}La_x)_2SiO_5$, $(Gd_{1-x}Eu_x)_2SiO_5$, and $(Gd_{1-x}Yb_x)_2SiO_5$, are attributed to the peculiarities of the electronic shell structures of lanthanum, europium, and ytterbium.

3. The diagram of thermodynamic stability for the $(Gd_{1-x}Ln_x)_2SiO_5$ systems and the domes of decomposition for the $(Gd_{1-x}Ln_x)_2SiO_5$ and $(Lu_{1-x}Ln_x)_2SiO_5$ systems are presented, allowing for graphical prediction of solid solutions decomposition temperatures based on given substitution limits, equilibrium substitution limits for given temperature, and ranges of thermodynamic stability.

4. The calculation results are consistent with the experimental literature data in the sense that the synthesis of single-phase samples

of solid solutions $(Gd_{1-x}Ln_x)_2SiO_5$ in studies [6–12, 14, 15, 17, 18] was conducted within the predicted regions of thermodynamic stability, while the synthesis of multiphase samples [13, 16, 38, 39] was carried out within the predicted regions of solid solution decomposition.

5. The majority of solid solution systems (8 out of 15) have critical decomposition temperatures below room temperature. Therefore, they may hold promise in the production of nanomaterials, as their synthesis typically requires relatively low temperatures.

6. Due to the very wide temperature range of thermodynamic stability, materials based on gadolinium oxyorthosilicate solid solutions may exhibit superior properties and reproducibility compared to materials based on oxyorthosilicates solid solutions of other REEs.

ACKNOWLEDGMENTS

The work of R.S., M.O., and G.E. was partially supported by the Programme of Fundamental Research funded by the Ministry of Education and Science of Ukraine (grant ID 0122U000762). R.S. expresses gratitude to the 'European Chemistry School for Ukrainians' project for the support provided.

REFERENCES

1. O. Ts. Sidletsky and B. V. Grynyov, *Stsyntylyatsiyni Krystaly na Osnovi Tverdykh Rozchyniv Zamishchennya* [Scintillation Crystals Based on Solid Substitutional Solutions] (Kharkiv: ISMA: 2019) (in Ukrainian); http://functmaterials.org.ua/contents/book/Book_Sidletskiy.pdf
2. S. Shimizu, K. Kurashige, T. Usui, N. Shimura, K. Sumiya, N. Senguttuvan, A. Gunji, M. Kamada, and H. Ishibashi, *IEEE Transactions on Nuclear Science*, **53**, No. 1: 14 (2006); doi:10.1109/TNS.2005.862975
3. V. Jarý, E. Mihokova, J. A. Mareль, A. Beitlerova, D. Kurtsev, O. Sidletskiy, and M. Nikl, *J. Phys. D: Appl. Phys.*, **47**, No. 34: 365304 (2014); doi:10.1088/0022-3727/47/36/365304
4. T. Usui, S. Shimizu, N. Shimura, K. Kurashige, Y. Kurata, K. Sumiya, N. Senguttuvan, A. Gunji, M. Kamada, and H. Ishibashi, *IEEE Transactions on Nuclear Science*, **54**, No. 1: 19 (2007); doi:10.1109/TNS.2006.886373
5. A. I. Slesarev, V. Ju. Ivanov, A. V. Ishchenko, A. N. Cherepanov, B. V. Shulgin, A. V. Chepkasova, and M. Kobajashi, *Working Substance for Thermo-Exoelectronic Dosimetry* (Patent RU 2331086 C1, IPC G01T 1/20, G01T 3/06 (2006.01). Application: 2007113282/28, 09.04.2007. Date of publication: 10.08.2008 Bull. 22); http://hdl.handle.net/10995/68666
6. P. Thiyagarajan, B. Tiwari, M. Kottaisamy, N. Rama, and M. S. Ramachandra Rao, *Appl. Phys. A*, **94**, No. 3: 607 (2009);

https://doi.org/10.1007/s00339-008-4861-z
7. Q. Wu, X. Jing, and H. Jiao, *Opt. Mater.*, **31**, No. 8: 1123 (2009); https://doi.org/10.1016/j.optmat.2008.12.004
8. L. H. Zheng, R. Lisiecki, Q. G. Wang, X. D. Xu, L. B. Su, W. Ryba-Romanowski, and J. Xu, *Lasers, Sources, and Related Photonic Devices* (OSA–Technical Digest (CD): Optica Publishing Group: 2012); https://doi.org/10.1364/AIOM.2012.IW3D.4
9. M. Jie, G. Zhao, X. Zeng, L. Su, H. Pang, X. He, and J. Xu, *J. Cryst. Growth*, **277**, Nos. 1–4: 175 (2005); https://doi.org/10.1016/j.jcrysgro.2004.12.160
10. D. Kurtsev, O. Sidletskiy, S. Neicheva, V. Bondar, O. Zelenskaya, V. Tarasov, M. Biatov, and A. Gektin, *Mater. Res. Bull.*, **52**: 25 (2014); https://doi.org/10.1016/j.materresbull.2014.01.006
11. V. V. Shinde, A. Tiwari, and S. J. Dhoble, *J. Mol. Struct.*, **1217**: 128397 (2020); https://doi.org/10.1016/j.molstruc.2020.128397
12. Yu. Zorenko, V. Gorbenko, V. Savchyn, T. Voznyak, B. Grinyov, O. Sidletskiy, D. Kurtsev, A. Fedorov, V. Baumer, M. Nikl, J. A. Mares, A. Beitlerova, P. Prusa, and M. Kucera, *J. Cryst. Growth*, **337**, No. 1: 72 (2011); https://doi.org/10.1016/j.jcrysgro.2011.10.003
13. S. N. Ogugua, S. K. K. Shaat, H. C. Swart, and O. M. Ntwaeaborwa, *J. Phys. Chem. Solids*, **83**: 109 (2015); https://doi.org/10.1016/j.jpcs.2015.04.002
14. S. N. Ogugua, S. K. K. Shaat, H. C. Swart, and O. M. Ntwaeaborwa, *J. Lumin.*, **179**: 154 (2016); https://doi.org/10.1016/j.jlumin.2016.06.056
15. M. Gao, P. Zhang, L. Luo, R. Guo, and Yu. Wang, *Optik*, **225**: 165814 (2021); https://doi.org/10.1016/j.ijleo.2020.165814
16. S. N. Ogugua, H. C. Swart, and O. M. Ntwaeaborwa, *Physica B*, **535**: 143 (2018); https://doi.org/10.1016/j.physb.2017.07.006
17. Ch. A. Rao and K. V. R. Murthy, *Int. J. Sci. Res. (IJSR)*, **10**, No. 1: 516 (2021); doi:10.21275/SR21110114938
18. H. Feng, J. Chen, Zh. Zhang, Y. Wang, Zh. Xu, J. Zhao, and R. Mao, *Radiat. Meas.*, **109**: 8 (2018); https://doi.org/10.1016/j.radmeas.2017.12.001
19. V. S. Urusov, *Teoriya Izomorfnoi Smesimosti* [The Theory of Isomorphous Miscibility] (Moskva: Nauka: 1977) (in Russian).
20. V. S. Urusov, *Fortschr. Mineral.*, **52**: 141 (1975).
21. V. S. Urusov, V. L. Tauson, and V. V. Akimov, *Geokhimiya Tverdogo Tela* [Geochemistry of Solid State] (Moskva: GEOS: 1997) (in Russian).
22. D. Spassky, A. Vasil'ev, V. Nagirnyi, I. Kudryavtseva, D. Deyneko, I. Nikiforov, I. Kondratyev, and B. Zadneprovski, *Materials*, **15**, No. 19: 6844 (2022); https://doi.org/10.3390/ma15196844
23. V. S. Voznyak-Levushkina, A. A. Arapova, D. A. Spassky, I. V. Nikiforov, and B. I. Zadneprovski, *Phys. Solid State*, **64**, No. 11: 567 (2022); https://doi.org/10.1134/S1063783422110130
24. E. I. Get'man, S. V. Radio, and L. I. Ardanova, *Inorg. Mater.*, **54**, No. 6: 596 (2018); https://doi.org/10.1134/S0020168518060031
25. R. D. Shannon, *Acta Crystallogr., Sect. A*, **32**, No. 5: 751 (1976); https://doi.org/10.1107/S0567739476001551
26. K. Li, and D. Xue, *J. Phys. Chem. A*, **110**, No. 39: 11332 (2006); https://doi.org/10.1021/jp062886k

27. J. Felsche, *The Crystal Chemistry of the Rare-Earth Silicates*. In: *Rare Earths. Structure and Bonding* (Berlin–Heidelberg: Springer: 1973), vol. **13**; https://doi.org/10.1007/3-540-06125-8_3
28. R. Becker, *Z. Metallkd.*, **29**: 245 (1937) (in German).
29. J. Wang, Sh. Tian, G. Li, F. Liao, and X. Jing, *Mater. Res. Bull.*, **36**, No. 10: 1855 (2001); https://doi.org/10.1016/S0025-5408(01)00664-X
30. E. G. Yukihara, L. G. Jacobsohn, M. W. Blair, B. L. Bennett, S. C. Tornga, R. E. Muenchausen, *J. Lumin.*, **130**, No. 12: 2309 (2010); https://doi.org/10.1016/j.jlumin.2010.07.010
31. R. E. Muenchausen, E. A. McKigney, L. G. Jacobsohn, M. W. Blair, B. L. Bennett, and D. W. Cooke, *IEEE Transactions on Nuclear Science*, **55**, No. 3: 1532 (2008); doi:10.1109/TNS.2008.922844
32. E. I. Get'man, Yu. A. Oleksii, S. V. Radio, and L. I. Ardanova, *Tonkie Khimicheskie Tekhnologii* [Fine Chemical Technologies], **15**, No. 5: 54 (2020); https://doi.org/10.32362/2410-6593-2020-15-5-54-62
33. S. S. Batsanov, *Strukturnaya Khimiya. Fakty i Zavisimosti* [Structural Chemistry. Facts and Dependences] (Moskva: Dialog-MGU: 2000) (in Russian).
34. S. S. Batsanov, *Russ. Chem. Rev.*, **37**, No. 5: 332 (1968); https://doi.org/10.1070/RC1968v037n05ABEH001639
35. R. Hoppe, *Adv. Fluor. Chem.*, **6**: 387 (1970).
36. B. Grynyov, V. Ryzhikov, J. K. Kim, and M. Jae, *Scintillator Crystals, Radiation Detectors & Instruments on Their Base* (Kharkiv: 2004); http://functmaterials.org.ua/contents/book/Ryzhikov-2004.pdf
37. E. I. Get'man and S. V. Radio, *Nanomaterials and Nanocomposites, Nanostructure Surfaces, and Their Applications. Springer Proceedings in Physics* (Eds. O. Fesenko and L. Yatsenko) (Springer: Cham.: 2021), vol. **246**; https://doi.org/10.1007/978-3-030-51905-6_39
38. S. N. Ogugua, R. L. Nyenge, P. T. Sechogela, H. C. Swart, and O. M. Ntwaeaborwa, *J. Vac. Sci. Technol. A*, **34**, No. 19: 021520 (2016); https://doi.org/10.1116/1.4942502
39. S. N. Ogugua, S. K. K. Shaat, H. C. Swart, R. E. Kroon, and O. M. Ntwaeaborwa, *J. Alloys Compd.*, **775**: 950 (2019); https://doi.org/10.1016/j.jallcom.2018.10.090
40. V. Y. Ivanov, V. A. Pustovarov, M. Kirm, E. S. Shlygin, and K. I. Shirinskii, *Phys. Solid State*, **47**, No. 8: 1492 (2005); https://doi.org/10.1134/1.2014499
41. K. Shakampally, P. M. Rao, and K. V. R. Murthy, *International Journal for Research in Applied Science & Engineering Technology (IJRASET)*, **5**, No. XI: 1735 (2017).
42. T. Utsu and S. Akiyama, *J. Cryst. Growth*, **109**, Nos. 1–4: 385 (1991); https://doi.org/10.1016/0022-0248(91)90207-L